

SLAC-PUB-4918

August 1989

(E)

**Transverse Electrodisintegration of the Deuteron  
in the Threshold Region at High  $Q^2$  \***

R. G. Arnold,<sup>(1)</sup> D. Benton,<sup>(1,a)</sup> P. E. Bosted,<sup>(1)</sup> L. Clogher,<sup>(1)</sup>  
G. Dechambrier,<sup>(1)</sup> A. T. Katramatou,<sup>(1)</sup> J. Lambert,<sup>(1,b)</sup> A. Lung,<sup>(1)</sup>  
G. G. Petratos,<sup>(1,c)</sup> A. Rahbar,<sup>(1)</sup> S. E. Rock,<sup>(1)</sup> Z. M. Szalata,<sup>(1)</sup>  
B. Debebe,<sup>(2)</sup> M. B. Frodyma,<sup>(2)</sup> R. S. Hicks,<sup>(2)</sup> A. Hotta,<sup>(2,d)</sup> G. A. Peterson,<sup>(2)</sup>  
R. A. Gearhart,<sup>(3)</sup> J. Alster,<sup>(4)</sup> J. Lichtenstadt,<sup>(4)</sup>  
F. Dietrich,<sup>(5)</sup> and K. van Bibber<sup>(5)</sup>

<sup>(1)</sup> *The American University, Washington, D.C. 20016 USA*

<sup>(2)</sup> *University of Massachusetts, Amherst, MA 01003 USA*

<sup>(3)</sup> *Stanford Linear Accelerator Center, Stanford University, Stanford, CA 94309 USA*

<sup>(4)</sup> *Tel Aviv University, Tel Aviv, Israel*

<sup>(5)</sup> *Lawrence Livermore National Laboratory, Livermore, CA 94550 USA*

**Abstract**

Cross sections for  $180^\circ$  deuteron electrodisintegration have been measured near threshold for the  $Q^2$ -range 1.21 to 2.77  $(\text{GeV}/c)^2$ . The new data, together with previous data (Ref. 2) at lower  $Q^2$ , show a change in slope near  $Q^2 = 1 (\text{GeV}/c)^2$ . Nonrelativistic calculations based on both meson-nucleon and hybrid quark-hadron models are not in quantitative agreement with the data over the entire  $Q^2$ -range. The ratio  $W_1/W_2$  of inelastic structure functions has been extracted using previous forward angle data and is found to decrease strongly near threshold.

Submitted to *Physical Review Letters*

---

\*This work was supported in part by Department of Energy contracts DE-AC03-76SF00515 (SLAC), W-7405-ENG-48 (LLNL), and DE-AC02-76ER-02853 (U. Mass.); National Science Foundation Grant PHY85-10549 (A.U.); and the U.S.-Israel Binational Science Foundation.

The deuteron is the most important nucleus for the study of the nucleon–nucleon interaction and the effects of meson exchange currents (MEC). Of particular interest is the transverse electrodisintegration of the deuteron, where a single magnetic transition to an unbound isospin triplet  $^1S_0$  state dominates the cross section near threshold. Existing data<sup>1,2</sup> are inconsistent with the diffraction minimum predicted in the impulse approximation (*IA*) at squared four-momentum transfer  $Q^2 \approx 0.5$  (GeV/c)<sup>2</sup>. The discrepancy is removed by MEC<sup>3-9</sup> and is the firmest evidence to date for their existence. The previous data extend to  $Q^2 = 1.1$  (GeV/c)<sup>2</sup>. At higher  $Q^2$ , theoretical predictions have been made within the meson–nucleon framework,<sup>4-6</sup> and using hybrid quark-hadron models.<sup>7-9</sup> In the latter, the deuteron is represented as a six-quark cluster when the *n-p* separation is comparable to or less than the nucleon size. These various approaches have resulted in order-of-magnitude differences in the cross sections predicted for  $Q^2 > 1$  (GeV/c)<sup>2</sup>.

In this Letter we present new measurements of threshold inelastic scattering from deuterium which more than double the  $Q^2$  range of previous data. The new data were obtained as a series of single-arm spectra of electron scattering near 180°. Double-arm measurements of elastic electron–deuteron scattering<sup>10</sup> were taken simultaneously with the single-arm data. The expected small cross sections made it necessary to use long liquid deuterium targets and a large acceptance spectrometer.

The experiment used electron beams of energy  $E = 0.734, 0.843, 0.885, 0.934, 1.020, 1.102, 1.201, \text{ and } 1.279$  GeV, produced by the Nuclear Physics Injector and the Stanford Linear Accelerator with a maximum intensity of  $5 \times 10^{11}$  electrons per 1.6  $\mu\text{sec}$  pulse at a rate of 150 Hz. Energy-defining slits limited the uncertainty in  $E$  to  $\pm 0.35\%$ . The beams were transported to a 180° spectrometer system<sup>11</sup>

in End Station A and directed into 10 or 20 cm liquid deuterium cells. Electrons scattered near  $180^\circ$  were momentum analysed using a set of six wire chambers. A large background of pions was rejected by a threshold gas Čerenkov counter and by measuring the energy deposited in an array of lead-glass blocks.

Radiatively corrected spectra at five incident beam energies are shown in Fig. 1. For each spectrum, the spectrometer central momentum  $E'$  was set at the deuteron elastic peak, and data were taken in the range  $\Delta E'/E' < \pm 3.5\%$ . This corresponds to an average range in  $E_{np}$  of  $\pm 35$  MeV, where  $E_{np}$  is the final state  $np$  kinetic energy. Corrections were applied for detector inefficiencies of 4% to 6%, dead-time losses of  $< 1\%$ , and contributions from target aluminum endcaps. The latter typically ranged from 10% at  $E_{np} = 30$  MeV to 100% for  $E_{np} < 0$ . The absolute solid angle<sup>11</sup> was evaluated to  $\pm 2\%$ . For  $E_{np} > 0$ , a correction of  $< 4\%$  for pions misidentified as electrons was performed by subtracting a scaled pion sample from each spectrum. Small elastic scattering contributions were also subtracted. The momentum calibration<sup>11</sup> of the electron spectrometer was evaluated using elastic scattering from hydrogen for low  $E'$  and detailed field maps of the bend magnets for the full range of  $E'$ . The resulting uncertainty in  $E'$  was  $\pm 0.25\%$ , which yields an error of  $\pm 10\%$  to  $\pm 30\%$  in the final cross sections. This was the dominant systematic error.

Radiative correction factors were obtained in the Mo and Tsai formalism<sup>12</sup> by convoluting theoretical cross sections<sup>4</sup> with a normalized bremsstrahlung shape. The uncertainty in the radiative correction factors was determined by performing the corrections separately for each of two input models with and without a large enhancement at  $E_{np} \approx 0$ . The resulting corrected cross sections varied by  $\pm 3\%$  to  $\pm 8\%$ .

Ionization losses, multiple scattering, and the spread in beam energy resulted in a resolution ranging from 12 to 20 MeV FWHM in  $E_{np}$ . In order to make a comparison with previous higher-resolution data and theoretical predictions, resolution effects have been taken into account using two methods. In the first method, theoretical models were convoluted with resolution functions calculated with a Monte-Carlo simulation<sup>13</sup> and compared with the data. All predictions shown in this Letter are nonrelativistic with the meson-nucleon models using the Paris potential.<sup>14</sup> Resolution-folded predictions are shown in Fig. 1. The curves represent calculations by Yamauchi<sup>8</sup> and Arenhövel.<sup>4</sup> The Yamauchi predictions are based on a hybrid quark-gluon and meson-nucleon degrees of freedom. They are in fair agreement with the data for  $E > 1$  GeV, but lie below the data at lower  $E$ . The calculations of Arenhövel use a meson-nucleon description with one and two-body exchange currents derived directly from the NN interaction. The present data lie between predictions using the Dirac electromagnetic form factor  $F_1(Q^2)$  for the MEC and those using the Sachs form factor  $G_E(Q^2)$ . The two predictions with  $G_E(Q^2)$  differ in the choice of electric neutron form factor,  $G_{En}(Q^2)$ , which also has a substantial effect.

Previous data<sup>1,2</sup> have generally been better described by models using  $F_1$ . This has motivated several theoretical arguments<sup>15</sup> in favor of its use. More recently, it has been pointed out<sup>16,17</sup> that both  $F_1$  and  $G_E$  can be justified in a nonrelativistic framework. It has also been shown<sup>16</sup> that substitution of a parametrized Bonn potential<sup>18</sup> with its relatively low D-state probability (4.8% compared to 5.8% for the Paris potential) can have as large an effect as the choice of  $F_1$  or  $G_E$ .

In the second method of comparing the present data with predictions and previous data, a model-dependent procedure was used to extract resolution-unfolded cross sections. In this method, the true cross section was represented by various models, convoluted with the resolution function, and then fit to the data. Polynomial models were chosen since they are consistent with the shape of available theoretical cross sections near threshold. The resulting unfolded spectra were then averaged over two ranges of  $E_{np}$ . Previous data have generally been averaged over 0 to 3 MeV. For the present data, large systematic errors in the unfolding procedure were dramatically reduced by averaging over larger ranges, 0 to 5 and 0 to 10 MeV. The error due to the uncertainty in  $E'$  was evaluated by shifting the data in momentum and performing a separate least-squares fit in each case. This yielded errors of  $\pm 35\%$  for the 10 MeV range to  $\pm 70\%$  for the 5 MeV range. Systematic errors due to the model dependence ranged from  $\pm 5\%$  (10 MeV range) to  $\pm 40\%$  (5 MeV range). An additional error of  $< \pm 5\%$  was due to the estimated uncertainty in the width of the resolution function. Final unfolded values were obtained as the centroid of the  $E_{np}$ -averaged cross sections resulting from various choices of model and momentum shift.

Resolution-unfolded data averaged over  $E_{np}$  from 0 to 10 MeV are shown in Fig. 2(a) with similarly averaged predictions by Yamauchi and Arenhövel. The quark model of Yamauchi is in good agreement with the data. Arenhövel's predictions using  $F_1$  and  $G_E$  differ by more than an order of magnitude, with the data lying between the two curves. These observations are consistent with those from Fig. 1. The  $IA$  result is shown for reference.

Resolution-unfolded cross sections averaged over  $E_{np}$  from 0 to 5 MeV are shown in Fig. 2(b) and 2(c) together with data below  $Q^2 = 1.2 \text{ (GeV/c)}^2$  from Ref. 2.

The data averaged over 0 to 5 MeV exhibit the same magnitude and slope as the more conservative 0 to 10 MeV results although the errors have grown considerably. The new data, together with the previous data at lower  $Q^2$ , indicate a distinct change in slope near  $Q^2 = 1 \text{ (GeV/c)}^2$ .

Several meson-nucleon models are shown in Fig. 2(b). As in Fig. 2(a), Arenhövel's models, here averaged over  $E_{np}$  from 0 to 3 MeV, lie above and below the data. These observations would not be affected if the calculations had been averaged from 0 to 5 MeV. Also shown is an earlier meson-nucleon model by Mathiot<sup>5</sup> at  $E_{np} = 1.5 \text{ MeV}$  with  $F_1$  coupling in the MEC. This model predicts a sharp diffractive minimum near  $Q^2 = 1.2 \text{ (GeV/c)}^2$  not seen in the  $E_{np}$ -averaged data.

Three predictions based on hybrid quark-hadron models<sup>7-9</sup> for  $E_{np} = 1.5 \text{ MeV}$  are shown in Fig. 2(c). The Yamauchi model has a diffractive minimum near  $Q^2 = 1 \text{ (GeV/c)}^2$  in disagreement with previous data, and the calculation of Cheng and Kisslinger,<sup>7</sup> obtained at  $155^\circ$ , lies above the present data. The prediction of Glozman<sup>9</sup> treats the quark-gluon and meson-nucleon degrees of freedom in a common harmonic oscillator basis using a coupled channels approach. This model shows fair agreement but needs to be extended above  $Q^2 = 1.5 \text{ (GeV/c)}^2$ .

All models beyond the  $IA$  shown in Fig. 2 are in qualitative agreement with the change in slope of the data near  $Q^2 = 1 \text{ (GeV/c)}^2$ . Interaction effects are clearly needed to shift the  $IA$  diffractive feature to higher  $Q^2$  and effectively fill it in. However, no model is in good agreement with the data over the full range of  $Q^2$ .

To gain further insight, the present  $180^\circ$  data which is dominated by transverse scattering can be compared to previous forward-angle data where the longitudinal cross section is dominant. The cross section can be written in terms of two structure

functions,  $W_1(E_{np}, Q^2)$  and  $W_2(E_{np}, Q^2)$ . The *IA* predicts that the ratio  $W_1/W_2$  at fixed  $Q^2$  should remain near unity as a function of  $E_{np}$ . Any deviations from this behavior may indicate the influence of interaction effects. The present threshold data and quasielastic data,<sup>19</sup> taken with the same apparatus, yield the resolution-unfolded  $W_1$  directly. Previous data<sup>20</sup> at  $8^\circ$ , essentially proportional to  $W_2$ , were also resolution-unfolded and interpolated to common values of  $E_{np}$  and  $Q^2$ .

The ratios  $W_1/W_2$  at three values of average  $Q^2$  are shown in Fig. 3. In each case  $W_1/W_2$  is approximately unity at large  $E_{np}$  but decreases as  $E_{np} \rightarrow 0$ , in agreement with earlier results<sup>21</sup> at lower  $Q^2$ . There are indications in Fig. 3 that the decrease is more gradual at higher  $Q^2$ , continuing a trend reported<sup>21</sup> at lower  $Q^2$ . The extracted values of  $W_1/W_2$  show that the quasifree mechanism is dominant above  $E_{np} \approx 50$  MeV in agreement with the *IA*. Near threshold, interaction effects are important over the full range of  $Q^2$ .

The curves in Fig. 3 represent calculations with final state interactions, MEC, and isobar configurations by Laget<sup>22</sup> and Arenhövel.<sup>4</sup> With the exception of Arenhövel's model using  $F_1$ , all calculations fail to reproduce the decrease in  $W_1/W_2$  observed near threshold. The choice of  $G_{En}(Q^2)$  has little effect on the predictions.

In summary, it has been found that threshold-inelastic cross sections measured at  $180^\circ$  show a change in slope near  $Q^2 = 1$  (GeV/c)<sup>2</sup>. Theoretical models based on divergent concepts are consistent with this trend, but quantitative agreement has yet to be achieved by any nonrelativistic model. The new cross sections at high  $Q^2$  as well as the extracted ratios  $W_1/W_2$  will provide a stringent test for relativistic models currently being developed.

## Acknowledgments

We would like to acknowledge the support of the SLAC staff. We would also like to thank H. Arenhövel, Y. Yamauchi and J. M. Laget for providing calculations at our kinematics.

## References

- (a) Present address: Princeton University, Princeton, NJ 08544
  - (b) Permanent address: Georgetown University, Washington, D.C. 20057
  - (c) Present address: University of Rochester, Rochester, NY 14423
  - (d) Permanent address: Shizuoka University, Shizuoka, 422 Japan
1. G. G. Simon *et al.*, Nucl. Phys. **A324**, 277 (1979); M. Bernheim *et al.*, Phys. Rev. Lett. **46**, 402 (1981); B. Parker, Ph.D thesis, University of Massachusetts, 1986.
  2. S. Auffret *et al.*, Phys. Rev. Lett. **55**, 1362 (1985).
  3. J. Hockert *et al.*, Nucl. Phys. **A217**, 14 (1973); J. A. Lock and L. L. Foldy, Ann. of Phys. **93**, 276 (1975).
  4. A. Buchmann *et al.*, Nucl. Phys. **A443**, 726 (1985); W. Leidemann and H. Arenhövel, Nucl. Phys. **A393**, 385 (1983); H. Arenhövel, Nucl. Phys. **A374**, 521c (1982), and private communication.
  5. J. F. Mathiot, Nucl. Phys. **A412**, 201 (1984).
  6. D. O. Riska, Phys. Scripta **31**, 107 (1985).
  7. L. S. Kisslinger, Phys. Lett. **112B**, 307 (1982); Tan-Sheng Cheng and L. S. Kisslinger, Nucl. Phys. **A457**, 602 (1986).
  8. Y. Yamauchi and M. Wakamatsu, Nucl. Phys. **A457**, 621 (1986); Y. Yamauchi *et al.*, Nucl. Phys. **A443**, 628 (1985), and private communication.
  9. L. Ya. Glozman *et al.*, Phys. Lett. **B200**, 406 (1988).
  10. R. G. Arnold *et al.*, Phys. Rev. Lett. **58**, 1723 (1987).

11. A. T. Katramatou *et al.*, Nucl. Instrum. Meth. **A267**, 448 (1988).
12. Y. S. Tsai, SLAC Report No. SLAC-PUB-848, 1971; L. W. Mo and Y. S. Tsai, Rev. Mod. Phys. **41**, 205 (1969).
13. A. T. Katramatou, SLAC Report No. SLAC-NPAS-TN-86-8, 1986.
14. M. Lacombe *et al.*, Phys. Rev. **C21**, 861 (1980).
15. J. Adam, Jr., and E. Truhlik, Czech. J. Phys. **B34**, 1157 (1984) and Few-Body System, Suppl. **1**, 261 (1986); J. Delorme, Nucl. Phys. **A446**, 65c (1985); E. Hadjimichael, Phys. Lett. **B172**, 156 (1986); J. M. Lina and B. Goulard, Phys. Rev. **C34**, 714 (1986).
16. H. Arenhövel, Prog. Theo. Phys. Suppl. **91**, 1 (1987); S. K. Singh *et al.*, Mainz preprint, MKPH-T-88-5.
17. F. Gross and D. O. Riska, Phys. Rev. C **36**, 1928 (1987).
18. R. Machleidt *et al.*, Phys. Rep. **149**, 1 (1987).
19. R. G. Arnold *et al.*, Phys. Rev. Lett. **61**, 806 (1988); G. G. Petratos, Ph.D thesis, The American University, 1988.
20. W. P. Schütz *et al.*, Phys. Rev. Lett. **38**, 259 (1977).
21. Yu. I. Titov, Kharkov preprint, KhFTI-87-38 and Int. Symp. on Lepton and Photon Interactions at High Energy, Hamburg, FRG (1987); A. S. Esausov *et al.*, Yad. Fiz. **45**, 410 (1987).
22. J. M. Laget, Phys. Lett. **199B**, 493 (1987); J. M. Laget, Can. J. Phys. **62**, 1046 (1984), and private communication.

## Figure Captions

Fig. 1. Electrodisintegration cross sections at  $180^\circ$  versus  $E_{np}$  for five values of the elastic  $Q^2$ . The error bars include statistical and systematic uncertainties. The predictions of Yamauchi (Ref. 8) and Arenhövel (Ref. 4) have been folded with the experimental resolution. Arenhövel's predictions are shown for  $F_1$  and two choices of  $G_E$  coupling in the MEC, as explained in the text.

Fig. 2. Threshold electrodisintegration cross sections at  $180^\circ$  versus  $Q^2$ . (a) Present data and meson-nucleon predictions of Arenhövel (Ref. 4) and hybrid quark-hadron predictions of Yamauchi (Ref. 8) averaged over  $E_{np}$  from 0 to 10 MeV. Arenhövel's predictions are shown for both  $F_1$  and  $G_E$  (with  $G_{En} \neq 0$ ) coupling in the MEC. Arenhövel's impulse approximation ( $IA$ ) is shown for reference. (b) Present data (solid circles) averaged over 0 to 5 MeV, along with previous data (open circles, Ref. 2), and meson-nucleon predictions of Arenhövel [same as (a)] averaged over 0 to 3 MeV. The meson-nucleon prediction of Mathiot (Ref. 5) is for  $E_{np} = 1.5$  MeV. (c) Data and Arenhövel's  $IA$  are the same as in (b). Hybrid quark-hadron predictions by Yamauchi (Ref. 8), Cheng and Kisslinger (Ref. 7), and Glozman (Ref. 9) are all for  $E_{np} = 1.5$  MeV.

Fig. 3. Extracted values of the ratio  $W_1/W_2$  versus  $E_{np}$  for three values of average  $Q^2$ . The inner error bars are statistical only, and outer error bars include systematic uncertainties. The predictions are by Arenhövel (Ref. 4, same as Fig. 2) and Laget (Ref. 22).

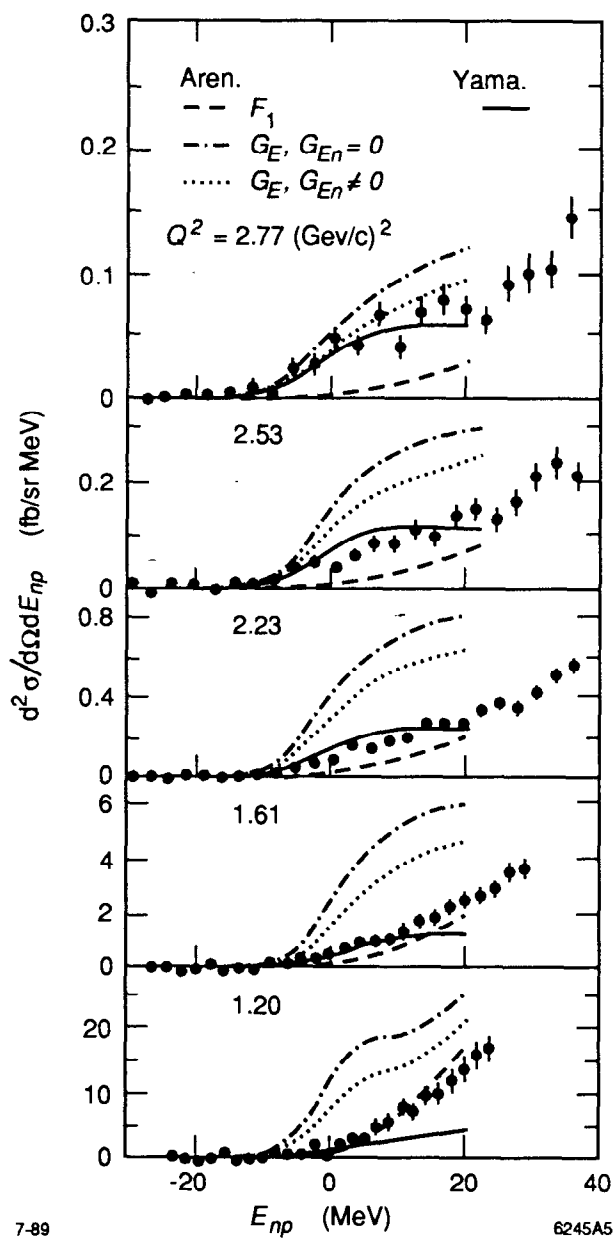


Fig. 1

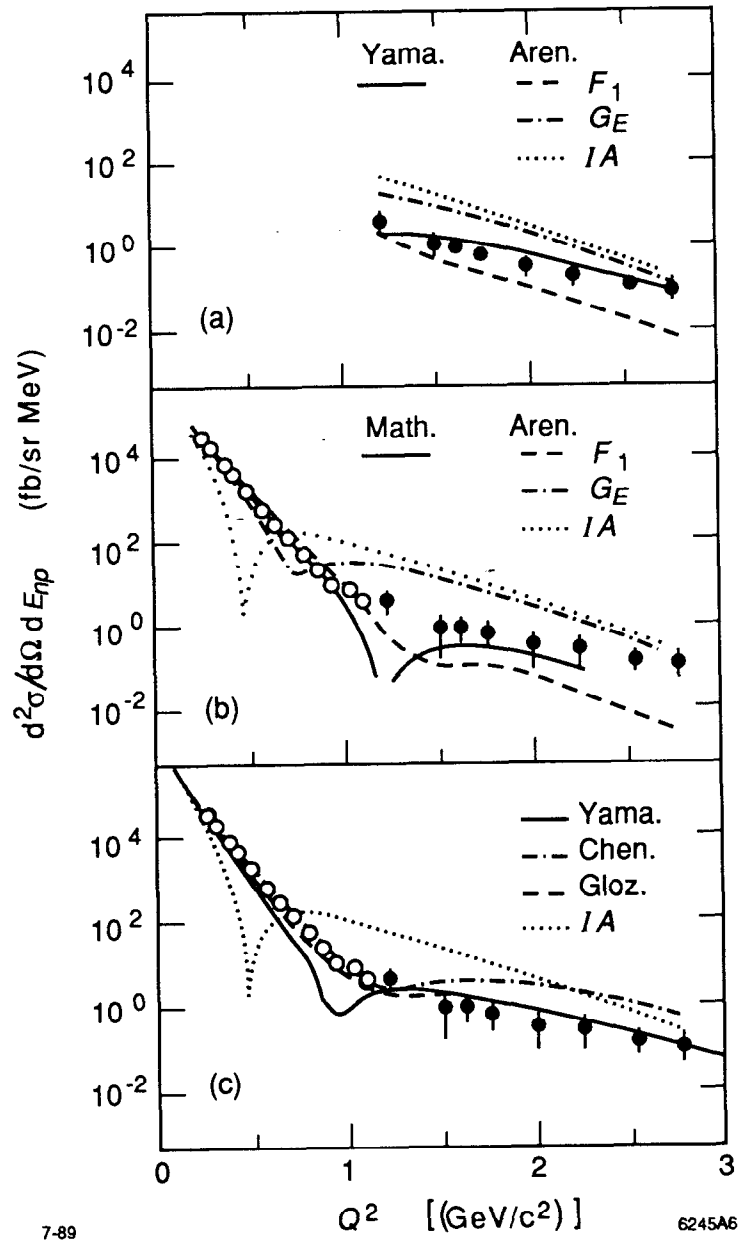


Fig. 2

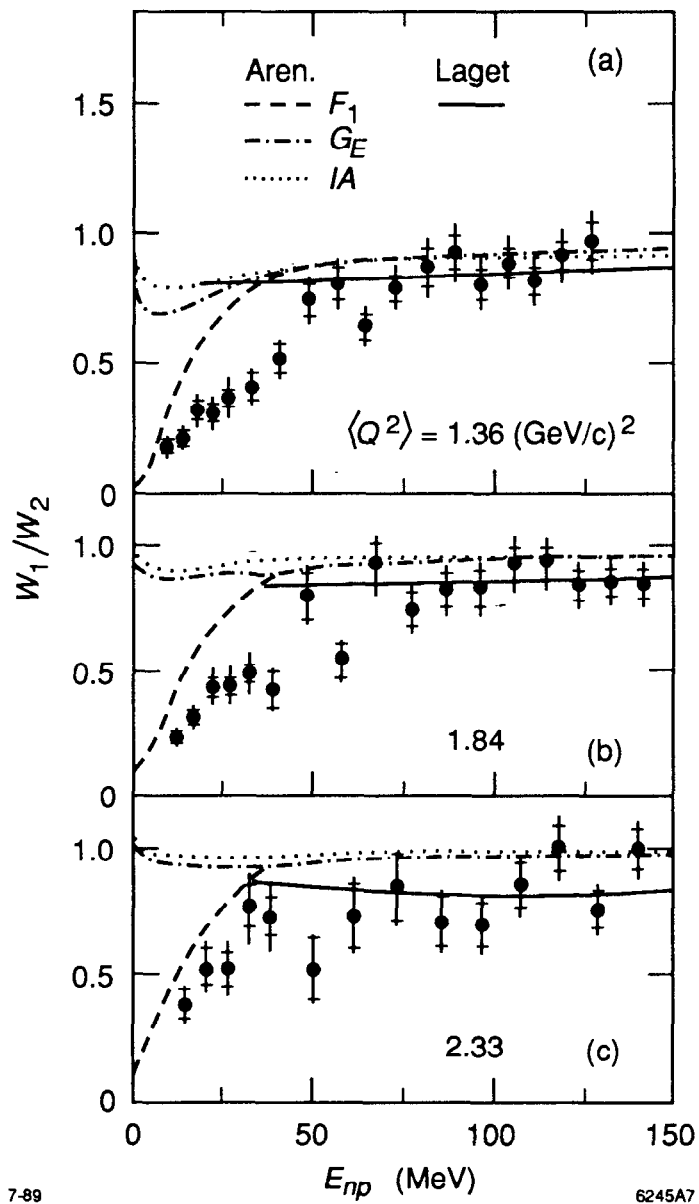


Fig. 3